Applied Physics Express

The Japan Society of Applied Physics

LETTER • OPEN ACCESS

Room-temperature Bloch oscillations and interminiband Zener tunneling in a GaAs-based narrow-minigap superlattice

To cite this article: Takeya Unuma *et al* 2021 *Appl. Phys. Express* **14** 081003

Applied Physics Express **14**, 081003 (2021) LETTER
https://doi.org/10.35848/1882-0786/ac114f

Room-temperature Bloch oscillations and interminiband Zener tunneling in a GaAs-based narrow-minigap superlattice

Takeya Unuma*, Yuto Itagaki, and Soichiro Asakura

Department of Electrical, Electronics and Information Engineering, Nagaoka University of Technology, Nagaoka, Niigata 940-2188, Japan

*E-mail: unuma@vos.nagaokaut.ac.jp

Received June 11, 2021; revised July 1, 2021; accepted July 4, 2021; published online July 14, 2021

We investigate peculiar Bloch oscillations and interminiband Zener tunneling in a GaAs-based narrow-minigap superlattice up to room temperature, by using terahertz emission spectroscopy under dc bias electric fields. The Bloch oscillations observed previously with a $\pi/2$ phase shift at 10 K under relatively low bias fields are found to survive even at 300 K, where thermal energy kT exceeds the relevant minigap (k: Boltzmann constant, T: temperature). Furthermore, the interminiband Zener tunneling under high bias fields leads to a monocyclic terahertz signal with a temperature-dependent subsequent bumpy tail, indicating its occurrence at a few different occasions for Bloch oscillating electrons.

Semiconductor superlattices (SLs) produce a variety of miniband structures in the original energy bands of host materials, leading us to in-depth understanding and sophisticated application of charge transport.[1–3] In the simplest case where a miniband is nearly isolated under dc bias electric field F, we have a Wannier–Stark ladder,[3–5] i.e. a series of equally separated energy levels with the mutual separation given by eFd for lattice constant d. Although electrons should be uniformly distributed onto the Wannier–Stark levels and cannot form any population inversion,[6] they have a voltage-tunable terahertz gain owing to scattering-induced energy broadening as revealed theoretically[7–10] and experimentally.[11–14] Our recent phase-sensitive measurements have shown that, when such electrons are created by femtosecond optical pulses, they exhibit terahertz Bloch oscillations (quantum beats) with a unique initial phase,[15–17] which reflects their capacitive nature equivalent to the occurrence of the steady-state inversionless gain,[14] up to above room temperature. Here, the uniform bias field normal to the SL layers is an underlying assumption; how to suppress field domains induced at high electron densities is a longstanding issue for the use of tunable terahertz gain in SL structures.[3,12]

It has been reported that the interminiband Zener tunneling[3,18–22] of electrons can be used as a key concept to prevent the formation of field domains and also coexist with tunable terahertz gain in doped narrow-minigap SLs, where the first miniband mixes substantially with higher minibands in the conduction band under bias field.[23–27] Very recently, we have discovered peculiar Bloch oscillations as well as interminiband Zener tunneling in an undoped narrow-minigap SL excited by femtosecond optical pulses at low temperatures of $T \leqslant 80$ K: the oscillation phase has a $\pi/2$ shift induced by interminiband mixing[28] and the dephasing time has a characteristic dependence on the excitation photon energy as explained by the miniband transport model,[29] in contrast to the Bloch oscillations reported for ordinary SLs with nearly isolated minibands.[14,15] However, the detailed properties of interminiband Zener tunneling, including its coexistence with Bloch oscillations at such temperatures that thermal energy kT (k: Boltzmann constant) exceeds the relevant minigap, have not yet been understood.

In this letter, we report temperature-dependent transient terahertz emission observed for a GaAs-based undoped narrow-minigap SL, with an emphasis on the properties of room-temperature Bloch oscillations and interminiband Zener tunneling. The oscillatory terahertz signal assigned to the Bloch oscillations in the conduction first miniband under relatively low bias fields was found to survive even at $T = 300$ K, where thermal energy kT exceeded the relevant minigap considerably, with the $\pi/2$ phase shift insensitive to temperature. Furthermore, the monocyclic terahertz signal under high bias fields was accompanied by a temperature-dependent subsequent bumpy tail, indicating that a majority of electrons underwent interminiband Zener tunneling on the first occasion and some others did so on a few later occasions during the Bloch oscillations in the conduction first miniband.

The sample prepared here was an undoped GaAs/$Al_{0.1}Ga_{0.9}As$ SL containing 59 periods, grown with well widths of 16.3 nm and barrier widths of 1.0 nm on an n^+-GaAs (001) substrate by molecular beam epitaxy. It was estimated by the Kronig–Penney model that the 14.8 meV wide first miniband was separated from the 47.9 meV wide second miniband by an 8.4 meV wide minigap in the conduction band.[28] The sample temperature T was systematically varied from 80 to 300 K, allowing thermal energy kT to go beyond the minigap midway. Electrons were created by $\sim$100 fs long near-infrared pulses at approximately the bottom of the first miniband under dc bias fields F applied in the growth direction. Here, we considered the known temperature-dependent band gap of the host material,[30] and adjusted the central photon energy at each temperature to make only a low energy part of the $\sim$20 meV wide pulse spectrum contribute to the interband optical excitation. The electron density was set to a relatively low value of $\sim 2 \times 10^{14}$ cm^{-3} so that it would hardly induce the field screening effect. We observed the temporal waveforms of terahertz emission from the sample by using a ZnTe (110) electro-optic crystal whose sensitivity was spectrally flat up to $\sim$3.5 THz and quenched above $\sim$4.0 THz. Other details of the experiment were similar to those reported in Refs. 15 and 29. The origin ($t = 0$) with an uncertainty of ±15 fs was given to the time axis of the observed terahertz waveforms by the maximum entropy method.[14,31,32]

The terahertz waveforms emitted at $T = 300$ K under different bias fields are shown in Fig. 1, with the excitation photon energy set to 1.427 eV. For the relatively low bias range where $F \lesssim 6.6\ \mathrm{kV\,cm^{-1}}$, we find that damped oscillations appear with a few cycles and have basic features identical to those of the Bloch oscillations observed previously with approximately $\pi/2$ phase shifts at low temperatures,[28,29] although thermal energy kT reaches 26 meV and substantially exceeds the minigap in the present situation. This indicates that electrons are hardly subjected to interminiband thermal excitation during their subpicosecond ballistic transport in the conduction first miniband. When the bias field is higher, the terahertz signal comes to have a monocyclic feature governed by the Zener tunneling into higher minibands.[28,29] Intriguingly, its relaxation from the negative peak observed for $F \simeq 11.5\ \mathrm{kV\,cm^{-1}}$ is significantly faster at 300 K than at low temperatures,[28,29] suggesting some thermally activated processes around the occurrence of interminiband Zener tunneling.

To understand the Bloch oscillations and interminiband Zener tunneling observed at room temperature, we examined the detailed temperature dependences of terahertz emission. The terahertz waveforms emitted under $F = 4.6\ \mathrm{kV\,cm^{-1}}$ at $T = 80$, 160, 240, and 300 K are shown by circles in Fig. 2(a), with the excitation photon energy set to 1.508, 1.485, 1.452, and 1.427 eV, respectively. Note that $T = 80$ K alone provides the case where thermal energy kT ($= 6.9$ meV) is lower than the minigap. The damping of the oscillatory terahertz signal is found to become somewhat faster with increasing temperature. We made a fitting analysis of the terahertz waveforms by following exactly the same procedure as described in Ref. 29, where the formula

$$J(t) = J_0 \Theta(t) e^{-\gamma t} \cos(\omega_B t + \alpha) \tag{1}$$

for transient current [J_0: magnitude, $\omega_B/2\pi$: resonance frequency, $1/\gamma$: dephasing time, α: initial phase, $\Theta(t)$: Heaviside

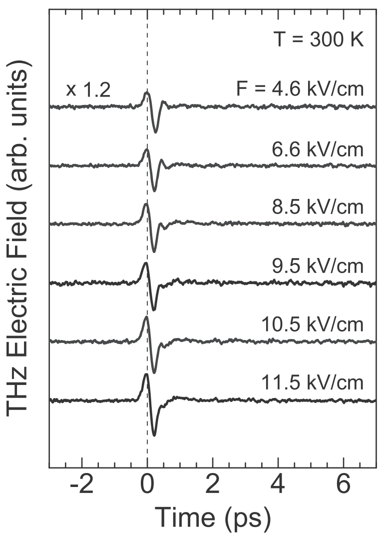

Fig. 1. Temporal waveforms of terahertz emission observed for a GaAs (16.3 nm)/$Al_{0.1}Ga_{0.9}As$ (1.0 nm) SL at room temperature ($T = 300$ K) under bias electric fields of $F = 4.6$–$11.5\ \mathrm{kV\,cm^{-1}}$. They are displayed with vertical offsets for clarity. Electrons were created by femtosecond optical pulses at approximately the bottom of the conduction first miniband.

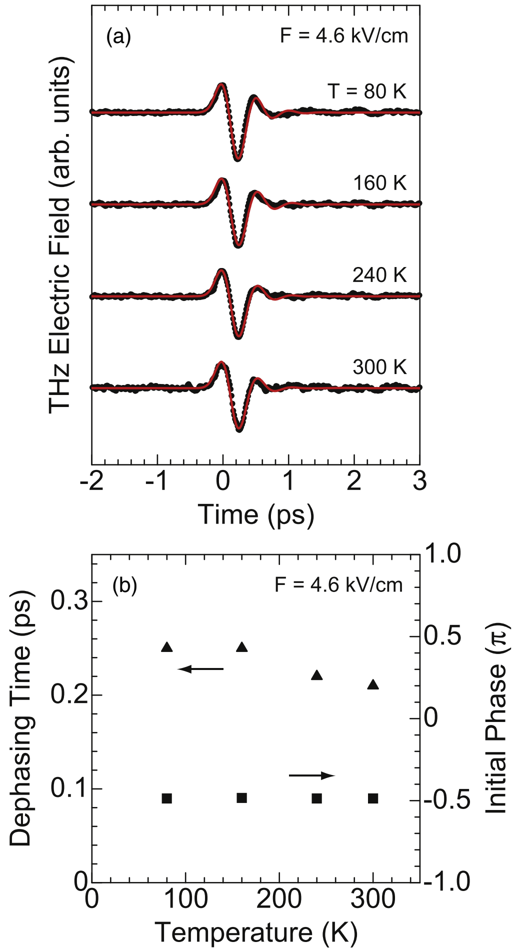

Fig. 2. (Color online) Terahertz waveforms emitted at various temperatures of $T = 80$–300 K under a relatively low bias electric field of $F = 4.6\ \mathrm{kV\,cm^{-1}}$. They are displayed with vertical offsets for clarity. Fitting analysis employing the formula for transient current given by Eq. (1) with a temporal resolution of 0.28 ps yielded (a) fits (curves) to the terahertz waveforms with resonance frequencies of $\omega_B/2\pi \simeq 1.9$ THz and also (b) dephasing time $1/\gamma$ (triangles) and initial phase α (squares) as adjustable parameters versus temperature.

step function] is employed to compute a fitting function for terahertz field, i.e. the convolution of dJ/dt with a temporal resolution of 0.28 ps that originates from the aforementioned measurement frequency bandwidth. We obtained the satisfactory fits shown by curves with resonance frequencies $\omega_B/2\pi$ almost equal to $eFd/h = 1.9$ THz.

The obtained sets of dephasing time $1/\gamma$ and initial phase α as adjustable parameters versus temperature are shown in Fig. 2(b). The dephasing time $1/\gamma$ has a constant value of 0.25 ps at $T = 80$–160 K (where thermal energy kT goes beyond the minigap with increasing temperature), indicating that the Bloch oscillating electrons do not directly receive the thermal energy. The decrease in $1/\gamma$ to 0.21 ps at higher temperatures can be ascribed to the more frequent scattering of the electrons by LO phonons through the Bose distribution factor.[16,33] Furthermore, the initial phase α takes approximately $-\pi/2$ at $T = 80$–300 K, in contrast to the values of $\alpha \simeq 0$ reported previously for nearly isolated minibands.[14,15] As we mentioned earlier, $\alpha \simeq -\pi/2$ (i.e. a $\pi/2$ phase shift) has been discovered also at low temperatures of $T \leqslant 80$ K,[28,29] together with the physical interpretation that electrons make a conductive response under substantial delocalization of their envelope wavefunctions due to interminiband mixing[28] (whereas $\alpha \simeq 0$ means a capacitive response[14,15]) under Wannier–Stark localization).

The terahertz waveforms emitted under $F = 11.5\,\mathrm{kV\,cm^{-1}}$ at the four different temperatures are shown in Fig. 3. The negative peak appearing at $t \simeq 0.2$ ps regardless of temperature can be ascribed to a series of events: a majority of electrons ballistically approach the Brillouin zone edge (i.e. $k_z = \pi/d$ in Refs. 28 and 29) with deceleration in the conduction first miniband (leading to negative values in the terahertz signal), undergo the Zener tunneling into various possible states of higher minibands, and stop a coherent contribution to the transient current (leading to the negative maximum in the terahertz signal). A pronounced feature seen at $T = 80$ K is the subsequent tail that extends to $t \simeq 1.0$ ps together with small bumps. These bumps have a period of ~0.25 ps, or a frequency of ~4.0 THz, which is at the high frequency limit of our electro-optic detection. Considering that $eFd/h = 4.8$ THz for $F = 11.5\,\mathrm{kV\,cm^{-1}}$, we assign the bumps to a low frequency part of the broad spectral peak expected for Bloch oscillations. Indeed, when reexamine similar bumps observed previously at $T = 10$ K,[29] we notice that they date back to the Bloch oscillations observed with $eFd/h < 4.0$ THz for lower bias fields.

This bumpy feature indicates that a minority of the electrons perform Bloch oscillations in the conduction first miniband for a while and experience interminiband Zener tunneling near the Brillouin zone edge on a few different occasions. The tail is found to become smaller and less bumpy with increasing temperature; this is presumably because phonon scattering[16] makes the Bloch oscillations dephased faster and also increases the minigap-dependent probability of interminiband Zener tunneling[18,28] effectively through the broadening of miniband edges. As a result, the relaxation from the negative peak is the fastest at $T = 300$ K. The terahertz signal turns slightly positive again at $t \simeq 0.7$–1.5 ps, perhaps owing to the incoherent transport of electrons accelerated by high bias field after interminiband Zener tunneling.

Here, we discuss the observed temperature dependence of terahertz emission in a few other aspects. First, recall that Bloch oscillating electrons have the in-plane degrees of freedom, which are not explicitly considered above. For the narrow-minigap SL at $T = 10$ K, we have reported that the dephasing time $1/\gamma$ decreases significantly with increasing excitation photon energy because the sum of the first miniband width and the in-plane excess energy for each electron goes beyond the LO phonon energy.[29] Figure 2(b) reveals a much weaker dependence of $1/\gamma$ on thermal energy kT, ruling out such a possible in-plane excess energy induced by thermal excitation during the subpicosecond ballistic transport. Second, let us refer to the possibility of intraminiband thermal excitation in ordinary SLs. For a nearly isolated 45 meV wide miniband, we have demonstrated that the terahertz emission due to Bloch oscillations exhibits no essential change when thermal energy kT goes beyond the energy separation eFd of a Wannier–Stark ladder.[15] However, it was unclear whether intraminiband thermal excitation occurred during the Bloch oscillations or not, because the Wannier–Stark ladder should be uniformly populated in either situation. Our findings obtained from the narrow-minigap SL suggest the latter situation. Finally, note that the terahertz emission in Fig. 2(a) nearly maintains its field strength up to room temperature, in contrast to that reported for ordinary SLs.[15] This is because the dephasing time $1/\gamma$ governs the field strength for $t > 0$ in both cases but presumably has a smaller contribution from LO phonon scattering[16,33] in the narrow-minigap SL with substantially delocalized electron wavefunctions.[28] The same trend is seen also for the terahertz emission in Fig. 3.

In summary, we studied the transient terahertz emission from a GaAs-based narrow-minigap SL for electrons created by femtosecond optical pulses at approximately the bottom of the conduction first miniband, varying both the dc bias electric field F and the sample temperature T. The oscillatory terahertz signal due to Bloch oscillations appeared for relatively low bias fields and was found to survive even at $T = 300$ K, where thermal energy kT exceeded the relevant minigap considerably. A fitting analysis showed that the electrons do not directly receive thermal energy kT during their subpicosecond ballistic transport in the conduction first miniband but are scattered by LO phonons more frequently near room temperature than at low temperatures through the Bose distribution factor; the oscillation phase is insensitive to temperature and also shifted by $\pi/2$ from those observed previously for nearly isolated minibands. Furthermore, the monocyclic terahertz signal due to the Zener tunneling into higher minibands appeared for high bias fields, together with a subsequent bumpy tail having a characteristic temperature dependence. This feature indicated that a majority of electrons undergo interminiband Zener tunneling on the first occasion and some others do so on a few later occasions during the Bloch oscillations in the conduction first miniband. Thus, we have offered a deeper understanding of ultrafast ballistic transport versus temperature, clarifying the intriguing properties of room-temperature Bloch oscillations and interminiband Zener tunneling.

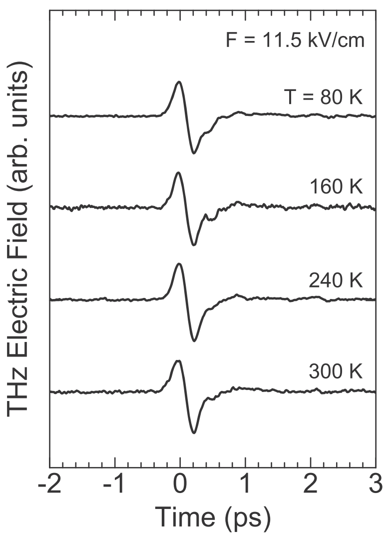

Fig. 3. Terahertz waveforms emitted at various temperatures of $T = 80$–300 K under a high bias electric field of $F = 11.5\,\mathrm{kV\,cm^{-1}}$. They are displayed with vertical offsets for clarity.

Acknowledgments We are grateful to Professor K. Hirakawa for providing one of us (T.U.) with the opportunity of fabricating the SL sample in his laboratory and also to Professor A. A. Andronov for exchanging information on recent progress with narrow-minigap SLs. This work was partly supported by JSPS KAKENHI Grant Numbers JP17H03232 and JP21H01362.

ORCID iDs Takeya Unuma https://orcid.org/0000-0002-4939-2194

1) L. Esaki and R. Tsu, IBM J. Res. Dev. **14**, 61 (1970).
2) M. Helm, Semicond. Sci. Technol. **10**, 557 (1995).
3) K. Leo, *High-Field Transport in Semiconductor Superlattices* (Springer, New York, 2003), p. 1, 87–150.
4) G. H. Wannier, Phys. Rev. **117**, 432 (1960).
5) M. Glück, A. R. Kolovsky, and H. J. Korsch, Phys. Rep. **366**, 183 (2002).
6) G. Bastard and R. Ferreira, C. R. Acad. Sci., Ser. II **312**, 971 (1991).
7) A. Wacker, Phys. Rev. B **66**, 085326 (2002).
8) H. Willenberg, G. H. Döhler, and J. Faist, Phys. Rev. B **67**, 085315 (2003).
9) F. T. Vasko, Phys. Rev. B **69**, 205309 (2004).
10) T. Unuma, N. Sekine, and K. Hirakawa, Appl. Phys. Lett. **89**, 161913 (2006).
11) Y. Shimada, K. Hirakawa, M. Odnoblioudov, and K. A. Chao, Phys. Rev. Lett. **90**, 046806 (2003).
12) P. G. Savvidis, B. Kolasa, G. Lee, and S. J. Allen, Phys. Rev. Lett. **92**, 196802 (2004).
13) N. Sekine and K. Hirakawa, Phys. Rev. Lett. **94**, 057408 (2005).
14) T. Unuma, Y. Ino, M. Kuwata-Gonokami, G. Bastard, and K. Hirakawa, Phys. Rev. B **81**, 125329 (2010).
15) A. Naka, K. Hirakawa, and T. Unuma, Appl. Phys. Express **9**, 112101 (2016).
16) T. Unuma and A. Matsuda, Appl. Phys. Lett. **112**, 162107 (2018).
17) T. Unuma, T. Hoshino, K. Nagahashi, and K. Ueda, Appl. Phys. Express **14**, 061003 (2021).
18) C. Zener, Proc. R. Soc. London Ser. A **145**, 523 (1934).
19) H. Schneider, H. T. Grahn, K. von Klitzing, and K. Ploog, Phys. Rev. Lett. **65**, 2720 (1990).
20) A. Sibille, J. F. Palmier, and F. Laruelle, Phys. Rev. Lett. **80**, 4506 (1998).
21) M. Helm, W. Hilber, G. Strasser, R. De Meester, F. M. Peeters, and A. Wacker, Phys. Rev. Lett. **82**, 3120 (1999).
22) B. Rosam, D. Meinhold, F. Löser, V. G. Lyssenko, S. Glutsch, F. Bechstedt, F. Rossi, K. Köhler, and K. Leo, Phys. Rev. Lett. **86**, 1307 (2001).
23) A. A. Andronov, I. M. Nefedov, and A. V. Sosnin, Semiconductors **37**, 360 (2003).
24) A. A. Andronov, E. P. Dodin, Y. N. Nozdrin, and D. I. Zinchenko, Phys. Status Solidi C **5**, 190 (2008).
25) A. A. Andronov, E. P. Dodin, D. I. Zinchenko, Y. N. Nozdrin, M. A. Ladugin, A. A. Marmalyuk, A. A. Padalitsa, V. A. Belyakov, I. V. Ladenkov, and A. G. Fefelov, JETP Lett. **102**, 207 (2015).
26) D. O. Winge, M. Franckié, and A. Wacker, AIP Adv. **6**, 045025 (2016).
27) A. A. Andronov et al., J. Phys.: Conf. Ser. **1189**, 012021 (2019).
28) T. Unuma and S. Maeda, Appl. Phys. Express **12**, 041003 (2019).
29) T. Unuma and R. Abe, Appl. Phys. Express **14**, 051009 (2021).
30) W. W. Chow and S. W. Koch, *Semiconductor-Laser Fundamentals* (Springer, Berlin, 1999), p. 197.
31) T. Unuma, Y. Ino, M. Kuwata-Gonokami, E. M. Vartiainen, K.-E. Peiponen, and K. Hirakawa, Opt. Express **18**, 15853 (2010).
32) T. Unuma, Y. Ino, K.-E. Peiponen, E. M. Vartiainen, M. Kuwata-Gonokami, and K. Hirakawa, Opt. Express **19**, 12759 (2011).
33) T. Unuma, M. Yoshita, T. Noda, H. Sakaki, and H. Akiyama, J. Appl. Phys. **93**, 1586 (2003).